What Can We Learn about the Solar Subsurface Large Scale Flows from Accurate High-Degree Modes Frequencies?

Helas VI — SOHO 28 — SPACEINN
Göttingen, GE

S.G. Korzennik

Harvard-Smithsonian Center for Astrophysics, USA.

September 2014

Contributors: A. Eff-Darwich (ULL, IAC)
T. Larson (Stanford)
M.C. Rabello-Soares (UFMG)
J. Schou (MPS)

Introduction

- High degrees "problem":
  - modes blend into ridges ($\ell > 200$, for p-modes, $\ell > 300$ for f-modes),
  - ridge characteristics (ν, A, Γ, α) are *not* the mode characteristics.

- Methodology
  - Fit ridges ($100 \leq \ell \leq 1000$),
  - Use multi-taper estimator (to reduce realization noise).
  - Apply a ridge to mode correction, based on *best* possible model of mode blending - dominated by the *effective* leakage matrix.
  - Iterate on model input parameters to best match observations.
  - Use the $100 \leq \ell \leq 300$ overlap for validation.

Coverage in the (ℓ, ν) Plane

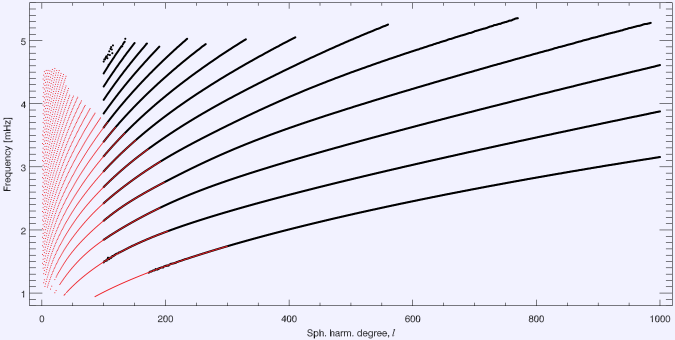

- Red dots: low and intermediate degrees: fitting resolved modes.
- Black circles: high degrees modes: ridge fitting.

Data Sets Analyzed

	2001 90 day long	2002 98 day long	2010 67 day long
MDI	$\surd$	$\surd$	$\surd$
GONG		$\surd$	$\surd$
HMI			$\surd$

- All epochs correspond to MDI *Dynamics* epochs.
- Can extend the time series for HMI & GONG.

Comparison with Resolved Modes

Year	Instrument	$\Delta\nu$ [μHz]	$\Delta\nu/\sigma_\nu$
2001	MDI	-0.220 ± 0.673	-0.880 ± 2.182
2002	MDI	-0.298 ± 0.966	-0.862 ± 2.631
	GONG	0.176 ± 0.769	0.517 ± 2.416
2010	MDI	-0.088 ± 1.087	-0.077 ± 2.766
	GONG	0.748 ± 1.186	2.751 ± 2.411
	HMI	0.269 ± 0.616	0.880 ± 2.044

- Mean and standard deviation of
  - frequency differences, and
  - frequency differences normalized by their uncertainties,

  between estimated mode frequencies derived from ridge fitting and coeval resolved mode frequencies measurements,
- for the $100 \leq \ell \leq 200|300$ overlapping range.

Comparison with Resolved Modes (cont'd)

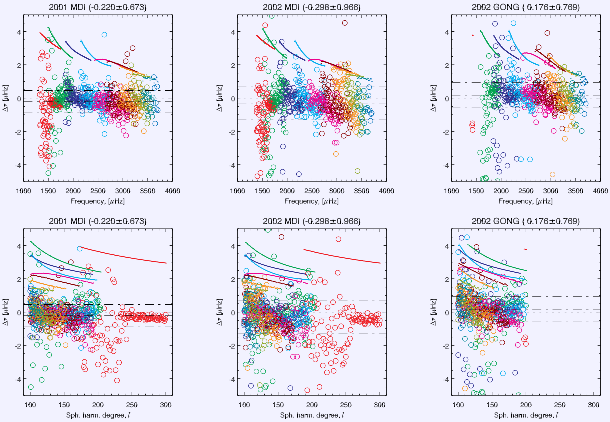

- Circles: frequency differences; dots: ridge to mode correction
- Differences are small, clustered near zero, with no discernible trends, and much smaller than the correction itself.
- The largest scatter is seen for the f-mode below $\ell = 250$ or so.

Comparison with Resolved Modes (cont'd)

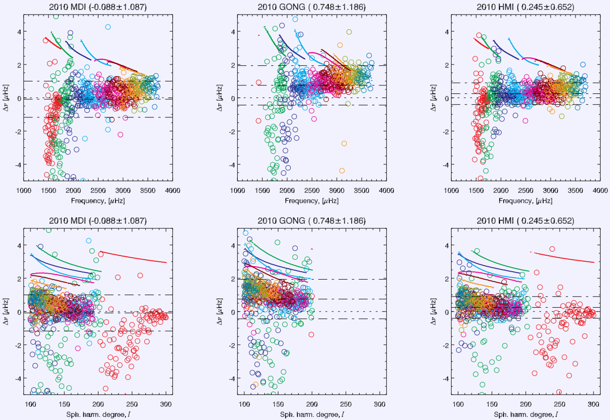

- Similar plot for MDI, GONG and HMI 2010.
- GONG comparison shows a larger bias (2.8σ)
- Scatter for the f-mode remains large even above $\ell = 250$.
- Is this the result of using a shorter time series? (67 versus 90 or 98 days).

Comparison at High Degree between Data Sets

Year	Instruments	$\Delta\nu$ [μHz]	$\Delta\nu/\sigma_\nu$
2002	GONG − MDI	-0.222 ± 0.460	-1.317 ± 1.470
2010	GONG − MDI	-0.982 ± 0.934	-4.260 ± 2.770
	HMI − MDI	-0.655 ± 1.117	-2.162 ± 1.572

- Mean and standard deviation of
  - frequency differences, and
  - frequency differences normalized by their uncertainties,
- between estimated mode frequencies derived from ridge fitting for different instruments and coeval epochs, with respect to MDI values.

Comparison of ν, Γ, & α, 2002

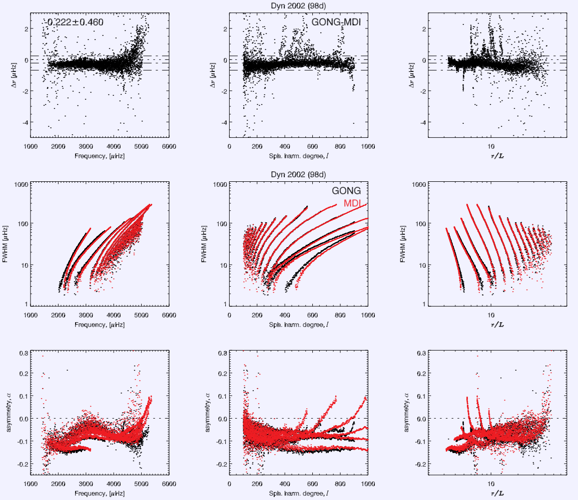

Comparison of ν, Γ, & α, 2010

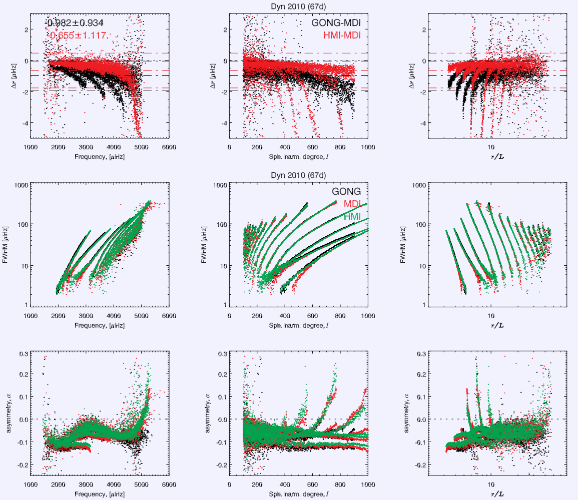

- By contrast with the 2002 data, the frequency comparison shows a variation with degree, and some dependence on frequency.

Comparison of Clebsch–Gordan Coefficients

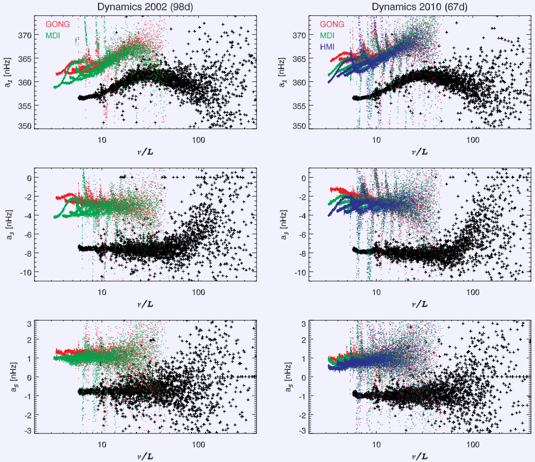

- Color dots: coefficients derived from ridge fitting.
- Black crosses: coefficients derived from coeval resolved mode fitting.

⇒ Large offset between ridge and mode estimate, and between instruments.

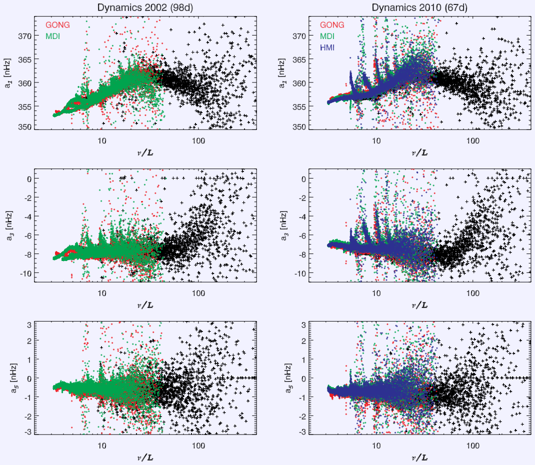

- Color circles: coefficients derived from mode estimates, after correcting ridge fitting results.
- Black crosses: coefficients derived from coeval resolved mode fitting.

⇒ Despite *horns*, both the offset high degree and mode estimate, and between instruments has vanished - no *ad hoc* fudging.

Rotation Inversions

- Inversion model grid (semi uniform in radius and latitude),
- shown in cartesian coordinates.

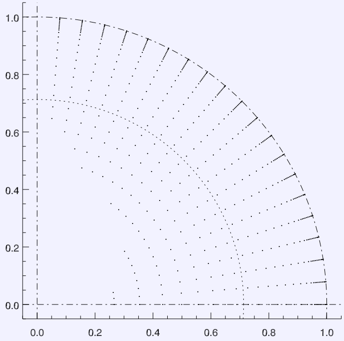

- A. Eff-Darwich inversion method.

Averaging Kernels

- Kernels for inversions using or not high degree modes (left vs right)

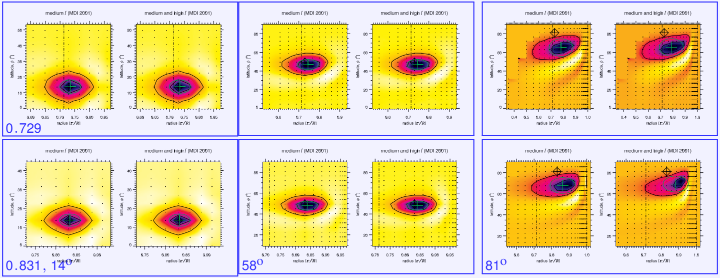

- Target location: black cross-diamond symbols,
- Kernel center of gravity and width: green crosses and circles.
- Inversion grid: black dots.

Averaging Kernels (Cont'd)

- Top 10%

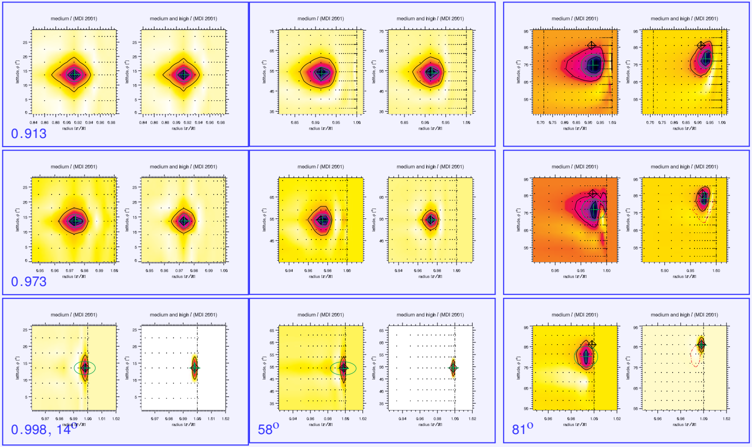

- Ratio of Γ_{ak} and differences Λ,
- for rotation inversions using or not high degree modes.

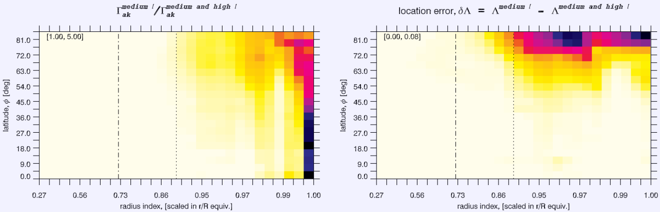

$$\Gamma_{ak} = \int K_a^2(r,\phi) D^2(r,\phi) dr d\phi / \int K_a^2(r,\phi) dr d\phi$$

$$\Lambda^2 = (r_t - r_c)^2 + ((\phi_t - \phi_c)/(\pi/2))^2$$

where $D^2 = (r - r_c)^2 + ((\phi - \phi_c)/(\pi/2))^2$, and (r_c, ϕ_c) is an estimate of the center of gravity of the averaging kernel main peak; and (r_t, ϕ_t) is the inversion target location on the solution grid.

Rotation Rate in the Outer 10% of the Solar Interior

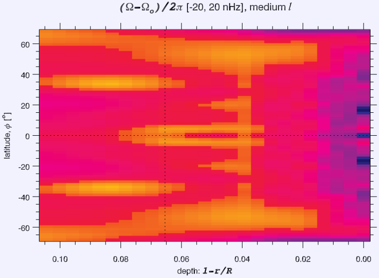

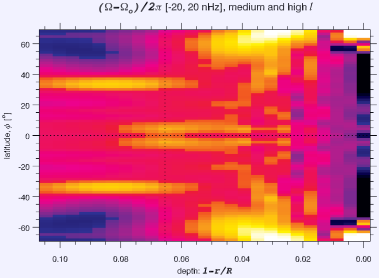

- after subtracting a differential rotation profile, inferred using or not high degree modes (right and left panels).

Note

- (a) the “torsonial oscillations” signal stands out more clearly when including high degrees, and
- (b) the profiles are quite different in the top 5%, esp. at high latitudes.

Medium-ℓ Only

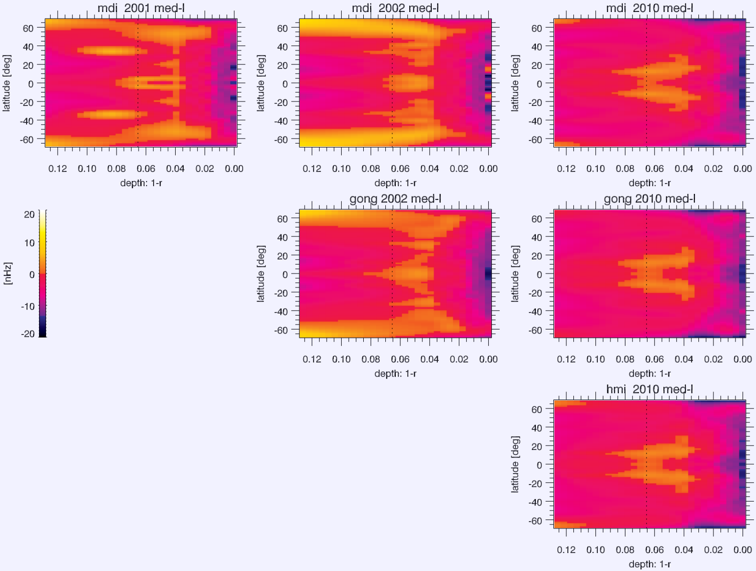

High- and Medium-ℓ

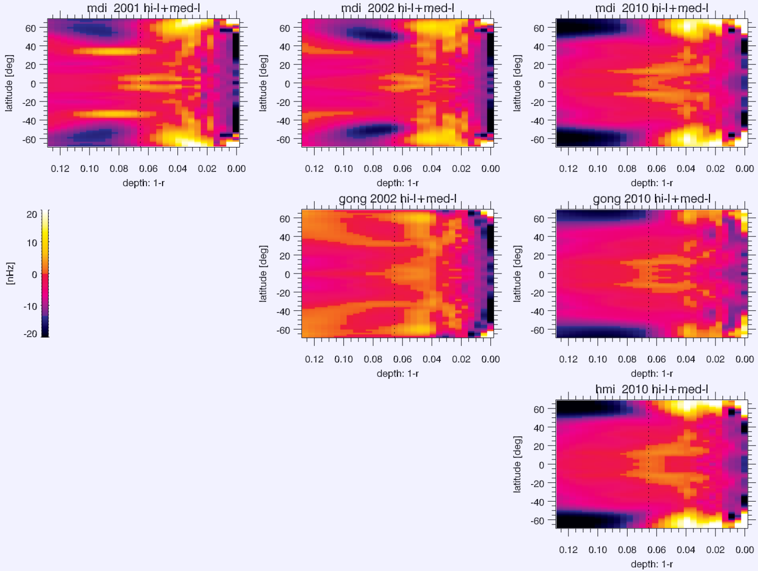

Conclusions

- Can use ridge values to estimate mode parameter.
- Discrepancies remains, likely due to short time series, error in PSF, ...
- GONG, MDI & HMI overlap can be leveraged to resolve this.
- Inclusion of high degree splittings affects solution in the top 10%,
  and alters the solution in the top 5%.
- Should produce and use high-degree mode estimates on a regular basis.

Tables are available at

`https://www.cfa.harvard.edu/~sylvain/research/`

under

`https://www.cfa.harvard.edu/~sylvain/research/tables/HiL/`

The End

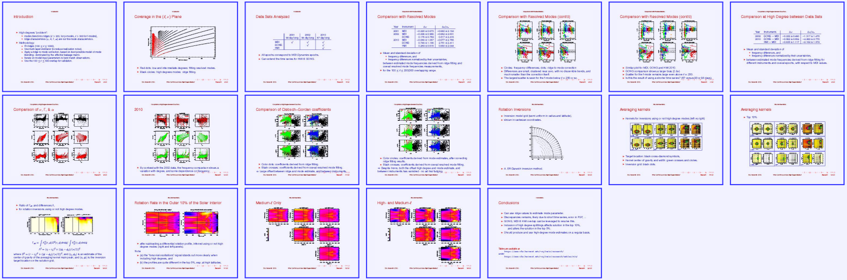
Introduction
Data Sets Analyzed
Comparison with Resolved Modes
Comparison with Resolved Modes (cont'd)
Comparison with Resolved Modes (cont'd)
Comparison at High Degree between Data Sets
2010
Comparison of Clebsch–Gordan coefficients
Rotation Inversions
Averaging kernels
Averaging kernels
Rotation Rate in the Outer 10% of the Solar Interior
High- and Medium-ℓ
Conclusions